

Particle Size Characterization through Bed Permeability Tests

Andrea C. Santomaso*, Elisabetta Carazzai, Silvia Volpato

APTLab – Advanced Particle Technology Laboratory – Dipartimento di Ingegneria Industriale, Università di Padova – via Marzolo 9, 35131 Padova, Italia
andrea.santomaso@unipd.it

This is an experimental study aiming at understanding the relationship between particle diameters measured with different analytical techniques: optical analysis (microscopy aided by computer image analysis), laser light scattering and permeability tests. Permeability test can provide an equivalent mean diameter that can be used in several cases where particle specific surface is the relevant property to focus on (for example problems related to particle reactivity or involving interactions with fluids as in pneumatic transport or in fluidization). This diameter can be determined by measuring the pressure loss in a granular bed of known porosity at various gas flow rate and by using a proper mathematical model (e.g., Darcy or Karman-Kozeny models) to correlate them. Four different materials (glass beads, granulated microcrystalline cellulose, MCC, sodium chloride crystals, tetraacetylenediamine powders, TAED) in the size range 700-1000 μm (by sieve analysis) were analysed. A strong discrepancy was observed by calculating the Sauter diameters from image analysis (and laser light scattering) and those from permeability measurements. The introduction of a function considering the pores morphology and connectivity was able to reconcile the size measured with the three different methods.

1. Introduction

Particle size definition is strongly dependent on the analytical method used to characterize the size. The use of equivalent particle diameters is normal in Particle Technology and the choice of one equivalent diameter rather than another should depend only on the specific application we are measuring the size for. However, the availability of a specific analytical instrument can determine the use of an incorrect equivalent diameter. Under this premise it can be useful to find some rule of equivalency between different equivalent particle diameters measured with different techniques. The results of this study can be of interest for processes involving packed or fluidized beds or where particle size is relevant (Tirapelle et al., 2021).

Studies on the flow of a viscous fluid through granular and porous media have mainly led to the derivation of macroscopic laws for fluid flow. The rate at which an interstitial fluid migrates through a granular and/or porous material under the effect of a pressure gradient is determined by permeability. This topic was first studied by Darcy who, for a creeping flow of a single-phase viscous fluid, experimentally derived the following phenomenological law:

$$\frac{\Delta P}{L} = \frac{\eta}{k} u_s \quad (1)$$

This law is known to hold for a wide variety of natural granular media ranging from loose sand to tight granite rocks. Here u_s is the superficial velocity of the fluid through the porous medium, η is the viscosity of the fluid, and P is the fluid pressure. The superficial velocity u_s has not to be confused with the interstitial velocity u_i defined as the volumetric flow rate divided by the cross-sectional area of the voids. So,

$$u_s = u_i \cdot \varepsilon \quad (2)$$

where ε is the void fraction or bulk porosity. The permeability coefficient, k , is a measure of fluid conductivity through the packed medium.

Eq(1) was put on a firmer theoretical basis for spherical monosized particles of diameter x by Kozeny and Carman who derived the result:

$$\frac{\Delta P}{L} = 180 \cdot \frac{\eta}{x^2} \cdot \frac{(1 - \varepsilon)^2}{\varepsilon^3} \cdot u_s \quad (3)$$

so that from Eq(1) and Eq(3):

$$k = \frac{x^2}{180} \cdot \frac{\varepsilon^3}{(1 - \varepsilon)^2} \quad (4)$$

For non monosized spherical particles the average Sauter diameter x_{32} must be used instead of x :

$$x_{32} = \frac{\sum f(x_i) \cdot x_i^3}{\sum f(x_i) \cdot x_i^2} \quad (5)$$

and for non-spherical particles the surface to volume equivalent diameter, x_{sv} , has to be used in the calculation of x_{32} . If different equivalent diameters are available (for example volume equivalent diameter, x_v , or surface equivalent diameter, x_s) a proper correction with particle sphericity, ϕ_s , needs to be used.

The prediction of the permeability k for various granular media has been a long-standing problem of great practical relevance. Several different experimental methods have been used in the studies from rather straightforward measurements to more sophisticated approaches, which utilize, e.g., mercury porosimetry, electrical conductivity, nuclear magnetic resonance, and acoustic properties of the medium. Theoretical work has often involved models with simplified pore geometries, which allows an analytical solution of the microscopic flow patterns. More sophisticated models based on statistical methods or on numerical simulations have also been used. However, due to the extremely complex nature of the phenomena involved, many basic questions remain unanswered. Various correlations between the permeability and the parameters describing the geometrical properties of the medium have been suggested, but a general form for the permeability as a function of bulk porosity is still lacking.

The flow resistance of a fluid percolating the porous sample can be experimentally evaluated by measuring the fluid rate in response to variations in the pressure drop or vice versa. Permeability constant is then obtained by fitting a predefined equation to the experimental data. In this work, permeability evaluation was based on Darcy Eq(1), to express the linear dependence of pressure drop (ΔP) through the medium with the resulting superficial velocity (u_s) where the linear term $[\eta u_s / k]$ in Darcy equation represents the viscous energy losses due to friction between fluid layers.

For incompressible flow (liquids) the pressure loss can be simply evaluated as:

$$\frac{\Delta P}{L} = \frac{P_1 - P_0}{L} \quad (6a)$$

and for compressible flow (gases and vapors) (Innocentini et al., 2010, 2019):

$$\frac{\Delta P}{L} = \frac{P_1^2 - P_0^2}{2PL} \quad (6b)$$

in which P_1 and P_0 are, respectively, the absolute fluid pressures at the entrance and exit of the medium, L is the packed bed length or thickness along the macroscopic flow direction, η and ρ are respectively the fluid viscosity and density. P is the pressure (either P_1 or P_0) for which u_s , η and ρ are measured or calculated. The superficial velocity u_s is the volumetric flow rate Q divided by the nominal surface area A of the sample exposed to flow. Due to the low-pressure drops experienced in the present experiment, the correction for compressible flow is very small (ΔP was only 0.2% higher for compressible flow at the highest flow velocity u_s). As reported in Nedderman (1994) measured values of the permeability and void fraction can be used as a means of determining the average particle diameter, x_{32} from Eq(2). This work aims exactly at investigating the possibility of using these types of measurements (permeability and bulk porosity) to estimate the size of the particles that form the granular bed when other analytical techniques are not available.

2. Materials and Methods

For the experimental evaluation of permeability, air at room temperature ($T = 20$ °C, $P = P_0 = 101325$ Pa, $\rho = 1.20$ kg/m³, $\eta = 1.81 \cdot 10^{-5}$ Pa s) was forced to flow through the granular sample at steady state in laminar regime. For laminar regime in a granular packed bed, Reynolds number should be smaller than 10:

$$Re = \frac{\rho u_s x}{\eta(1-\varepsilon)} < 10$$

The sample powder was poured in a hollow cylinder and sandwiched between two horizontal fine grids (see Figure 1). Table 1 gives a description of the sample geometry and dimensions.

Table 1: Packed granular bed geometry.

Sample diameter	Sample length	Cross flow area	Sample volume
D [m]	L [m]	A [m ²]	V [m ³]
0.059	0.053	$2.73 \cdot 10^{-3}$	$1.45 \cdot 10^{-4}$

Below the sample, an expansion chamber at pressure P_1 allowed the even distribution of the air through the packed bed. The flow was controlled by valves and measured with different rotameters. Three rotameters were used for different ranges of flow rate as schematized in Figure 1.

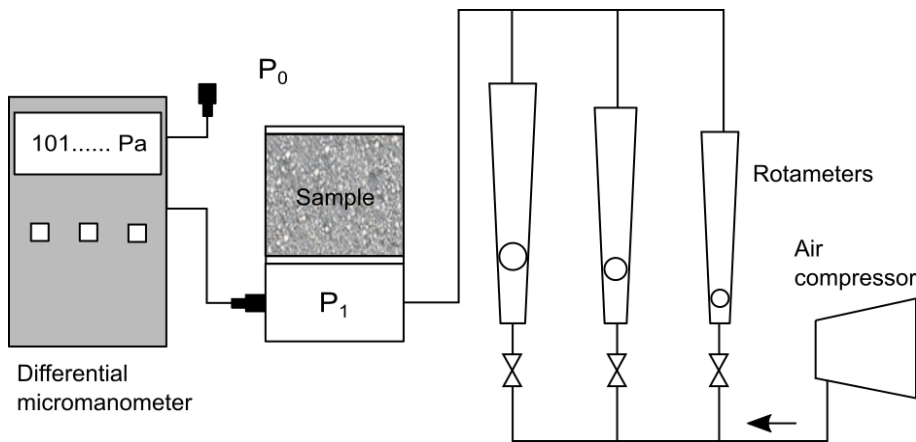


Figure 1: Experimental set-up for permeability tests.

Pressure drop ΔP was measured with a digital micromanometer (Bluetooth testo 510i, Testo SpA) and recorded as a function of the air volumetric flow rate Q , measured with a rotameter. Q was then converted to the superficial velocity by $u_s = Q/A$. The collected data set (ΔP vs. u_s) was fitted according to the least-square method using a liner model of the type: $\Delta P/L = m \cdot u_s$. The permeability parameter of Darcy equation in Eq(1) was then calculated from the fitting constant m as $k = \eta/m$.

Care was given to the creation of the packed bed. The cylinder was filled simply pouring the powder in the cylinder or by pluviation from different heights or by tapping the cylinder after filling it to obtain beds with different packing porosity. Eq(3) was rearranged and used to calculate the diameter $x_{\Delta P}$ as:

$$x_{\Delta P} = \left[180 \cdot \eta \cdot \frac{(1-\varepsilon)^2}{\varepsilon^3} \cdot \frac{1}{\frac{1}{u_s} \frac{\Delta P}{L}} \right]^{0.5} \quad (7)$$

ε and the group $1/u_s \cdot \Delta P/L$ in this equation are measured quantities and $x_{\Delta P}$ with subscript ΔP indicates that the diameter comes from permeability tests.

Four different materials (glass beads, granulated microcrystalline cellulose, MCC, sodium chloride crystals, tetraacetylenediamine powders, TAED) in the size range 700-1000 μm (by sieve analysis) have been analysed. Particles had similar size but where different for particle shape and surface roughness (Figure 2). For comparing permeability test results, the size of the particles was measured also by optical microscopy and Image Analysis (IA) and by Laser Light Scattering, LLS (Malvern Hydro 2000, Malvern, UK). Images were analysed with the software Fiji (Schindelin et al., 2012). The Sauter mean diameters x_{32} , were then calculated from the particle size distributions (PSDs) obtained from the two methods and are here indicated as x_{IA} and x_{LLS} respectively.

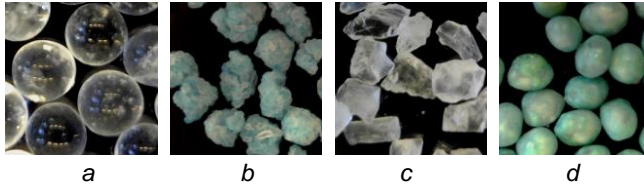


Figure 2: Powder used for the tests: a. glass beads, b. TAED powders, c. Salt (NaCl), d. granulated MCC.

3. Results and Discussion

Results and discussion

It is clear from Eq(7) that for the same granular material (made of particles with the same size) different diameters $x_{\Delta P}$ can be calculated as a function of bulk porosity simply by changing the packing level of the granular bed. The same powder, packed in different ways (i.e., with different ϵ), appears to be made of particles with different average size. Figure 3 shows the trend of $x_{\Delta P}$ vs ϵ .

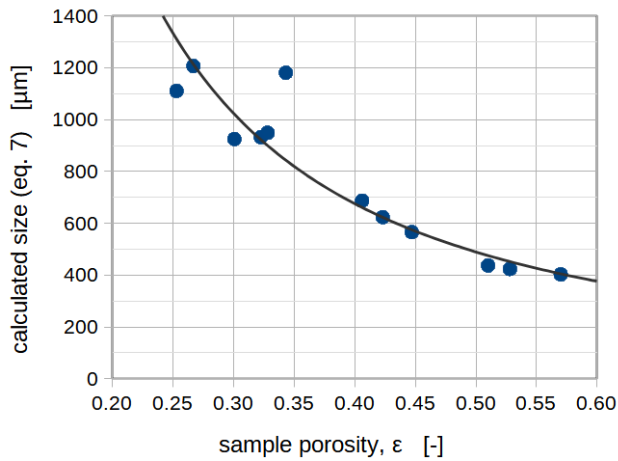


Figure 3: Particle size calculated from permeability test results using Eq(7).

Table 3: Bulk porosity, circularity ($\phi_c = [4\pi A_p]^{0.5}/P$) and particle sizes estimated using the different methods.

Material	Porosity, ϵ [-]	Particle circularity, ϕ_c [-]	$x_{\Delta P}$ from Eq(4) [μm]	x_{IA} from IA (number based) [μm]	x_{LLS} from LLS (mass based) [μm]	x_{IA} from IA (mass based) [μm]
MCC	0.253	0.93	1111	594	588	661
	0.267		1206			
	0.301		925			
	0.322		932			
	0.328		949			
Glass beads	0.343	0.98	1181	873	955	900
Salt	0.406	0.71	687	610	941	989
	0.423		623			
	0.447		566			
TAED	0.510	0.74	437	629	920	1001
	0.528		423			
	0.570		402			

Table 3 shows the measurements/calculations performed with the materials at different porosities according to Eq(7) and compares them with the sizes measured IA and those measured LLS. A direct correspondence was found between Sauter mean diameter x_{32} calculated from IA and LLS data after transformation of IA PSD from number to mass basis. While there was an agreement between these two diameters a large discrepancy was observed with the diameters calculated from permeability tests. For most of the materials, the calculated diameter was smaller than the measured one (glass beads, salt and TAED powders), *viceversa* for the granulated MCC.

The diameter $x_{\Delta P}$ calculated by Eq(7) has therefore to be interpreted as an average equivalent diameter which has not a direct correspondence with the physical dimension of the particle that constitute the granular packing since it is strongly affected by morphology, size distribution, connectivity and volume of the void fraction (bulk porosity).

In order to make the particle diameter constant (for each type of material) and equal to that measured by IA we need to modify Eq(3) or Eq(7) by substituting the constant $C = 180$ in Eq(7) with a function of bulk porosity $f(\varepsilon)$. Let's therefore rewrite Eq(7) as:

$$x_{IA} = \left[36 \cdot f(\varepsilon) \cdot \eta \cdot \frac{(1 - \varepsilon)^2}{\varepsilon^3} \cdot \frac{1}{\frac{1}{u_s} \frac{\Delta P}{L}} \right]^{0.5} \quad (8)$$

where the constant $C = 180$ has been substituted with $36 \cdot f(\varepsilon)$. The function $f(\varepsilon)$ has the scope of preserving the independence of the diameter on ε and considers all the complexity of the bed packing (morphology and connectivity of the pores). From Eq(8) this function can be made explicit and then plotted in Figure 4.

$$f(\varepsilon) = \frac{x_{IA}^2}{36} \cdot \frac{1}{u_s} \cdot \frac{\Delta P}{L} \cdot \frac{1}{\eta} \cdot \frac{\varepsilon^3}{(1 - \varepsilon)^2} \quad (9)$$

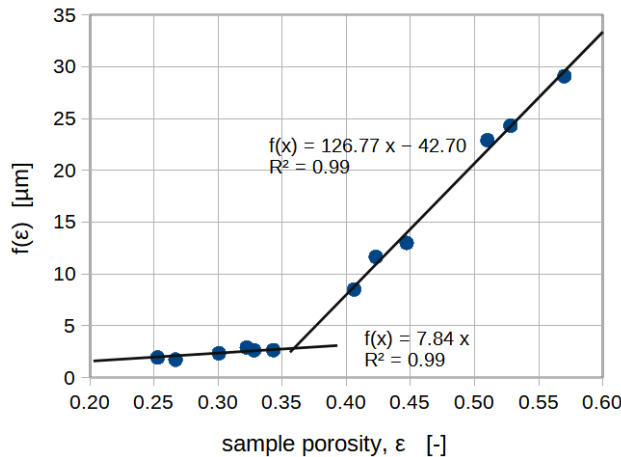


Figure 4: Determination of the function $f(\varepsilon)$ by linear fitting.

From Figure 4 it can be observed that $f(\varepsilon)$ can be fitted (least-square method) by two linear functions with a very high coefficient of determination ($R^2 = 0.99$). Their expressions are:

$$f(\varepsilon) = 7.84 \cdot \varepsilon \quad \text{for } \varepsilon < 0.36 \text{ and } \phi_c > 0.90 \quad (10a)$$

$$f(\varepsilon) = 126.77 \cdot \varepsilon - 42.70 \quad \text{for } \varepsilon > 0.36 \text{ and } \phi_c < 0.90 \quad (10b)$$

The group $36 \cdot f(\varepsilon)$ spans in the range 60-1000 (with the present experiments) and can be therefore very different from the constant C of Carman-Kozeny equation which is invariably 180. It can be observed looking at Table 3 that particles with circularity $\phi_c > 0.90$ fit to Eq(10a) while those with $\phi_c < 0.90$ fit to Eq(10b) suggesting also a dependence of bulk porosity on particle shape. By applying the function $f(\varepsilon)$ into Eq(8) allows to correct the diameter obtained from permeability tests and to make it very similar (as values) to the one estimated by IA. Figure 5 shows a parity plot of the diameters from permeability tests vs the IA diameters before and after correction (by using $f(\varepsilon)$). The improvement of the estimated diameters is self-evident.

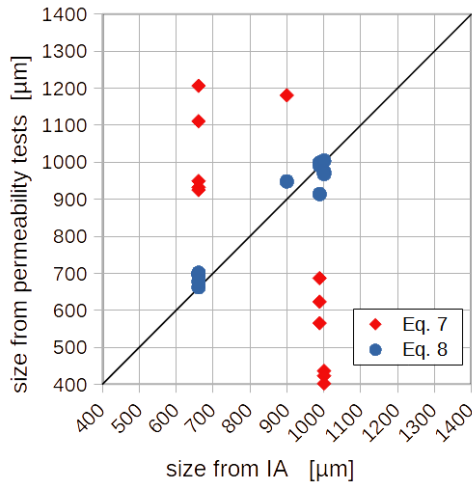


Figure 5: Parity plot comparing the particle sizes obtained from permeability tests (estimated with Eq(7) and Eq(8) respectively) with those obtained from microscopy assisted by computer image analysis.

Clearly, these results are affected by the limited number of materials tested and further experiments needs to be collected, however the trend is clear and only minor modifications on the fitting functions are expected.

4. Conclusions

Particle diameters measured with different analytical techniques have been compared. Optical analysis (microscopy aided by computer image analysis) and laser light scattering have shown agreement between them while permeability test result deviated from the former. Only the introduction of a function of the bulk porosity was able to reconcile the size measured with the three different methods. The dependency of this function on the bulk porosity suggests that pores morphology and connectivity (i.e., the tortuosity) can be involved and further studies are required to define this dependence. Nevertheless, the results obtained here allow permeability measurements to be used to directly determine the actual average particle size as it would be measured by optical microscopy or laser light scattering techniques.

Nomenclature

A – cross sectional area of the sample, m^2
 k – permeability coefficient, m^2
 L – sample thickness, m
 m – slope from fitting, $m^2/(Pa \cdot s)$
 P – pressure, Pa
 Q – air flow rate, m^3/s
 T – air temperature, $^{\circ}C$
 u_i – interstitial velocity, m/s

u_s – superficial velocity, m/s
 x – generic particle diameter, m or μm
 x_{32} – generic Sauter mean diameter, m or μm
 x_{IA}, x_{LLS} – diameter from IA, LLS, m or μm
 ε – sample porosity, -
 ϕ_s, ϕ_c – particle sphericity, circularity -
 η – air viscosity, $Pa \cdot s$
 ρ – air density, kg/m^3

References

- Innocentini M.D.M., Faleiros R.K., Pisani Jr R., Thijs I., Luyten J., Mullens S., 2010, Permeability of porous gelcast scaffolds for bone tissue engineering, *Journal of Porous Materials*, 17(5), 615–27.
 Innocentini M.D.M., Faria M.A.V., Crespi M.R., Andrade V.H.B., 2019, Air Permeability Assessment of Corrugated Fiber-Cement Roofing Sheets, *Cement and Concrete Composites* 97, 259–67.
 Nedderman R.M., 1992, *Statics and kinematics of granular materials*, Cambridge University Press.
 Tirapelle M., Troncon L., Volpato S., Santomaso A.C., 2021, Size Segregation of Ternary Mixtures in Inclined Chute Flows: an Experimental Study, *Chemical Engineering Transaction*, 86, 823-828
 Schindelin J., Arganda-Carreras I., Frise E., Kaynig V., Longair M., Pietzsch T., Cardona A., 2012, Fiji: an open-source platform for biological-image analysis. *Nature Methods*, 9(7), 676–682.